COLLEGE OF ENGINEERING

REPORT # 139

College of Engr. Report #139

Reprinted from THE JOURNAL OF THE ACOUSTICAL SOCIETY OF AMERICA, Vol. 45, No. 5, 1166–1179, May 1969

Theory of Holographic Interferometry

G. M. BROWN, R. M. GRANT, AND G. W. STROKE*

GC Optronics, Inc., Ann Arbor, Michigan 48104

A simple theory of three forms of holographic interferometry—"time-average," multiple-exposure, and "real-time" (live) interferometry—is presented, based on a new development in holographic "image synthesis" (complex amplitude addition and subtraction), introduced in 1965 by D. Gabor and G. W. Stroke *et al.* They demonstrated the remarkable property of holography: Interference can occur between two or more light beams that are not superimposed either in time or in space, if the holographic intensities corresponding to the beams are obtained with the aid of a coherent reference-background beam of the same spatial shape and if these intensities are successively added in the same hologram. Following the independent discovery of holographic interferometry, in 1965, by J. M. Burch; by R. L. Powell and K. A. Stetson; and by L. O. Heflinger, R. F. Wuerker, and R. E. Brooks, among others, it was found that two or more successive photographic additions of the hologram intensities (corresponding to two or more *sequential* positions or shapes of a given object) would thus indeed permit one to "synthesize," in the form of an interferogram, the complex sum of the spatial-electric-field vectors, corresponding to each object-point position, as if the different object-point positions had all existed *simultaneously* rather than sequentially, as they do during the hologram recording (for instance in the case of multiple holographic-image recording of a vibrating object). The rigorous equations we present, notably in vector form, for the general cases of practical interest bear out the equations previously derived by a number of authors, for some special cases, frequently in heuristic form.

INTRODUCTION[1–6]

If Lord Rayleigh could revisit Earth today, he would no doubt be pleased to find that holographically obtained interferograms of the topology of vibrating acoustical transducers may have indeed introduced a surprising new element into acoustics, in spite of his famous statement (p. 141, Vol. 2, 1898 edition of his *Theory of Sound*[7]): "The diffraction of sound is a subject which has attracted but little attention either from mathematicians or experimentalists. Although the general character of the phenomena is well understood, and therefore no very startling discoveries are to be expected, the exact solution of a few of the simpler problems which the subject presents, would be interesting, . . ."

It is almost certain that Lord Rayleigh would stress the importance of the new possibility (now becoming available) to solve even quite complicated problems in acoustical diffraction, with the aid of holographically obtained, detailed, interferometric measurements of the topology of the displacement of the entire surface of a vibrating transducer. From these measurements, one could determine the detailed, over-the-surface, pressure- and velocity-field distributions, which are required to determine the diffracting characteristics of the transducer and notably its "directivity," farfield, or other diffraction patterns.

Indeed, Lord Rayleigh would probably appreciate the possible rôle of holographic interferometry in acoustics as "startling" in terms of another remark he made (on p. 140 of his treatise): "The expression of P and ϵ [i.e., of the parameters characterizing the spatial derivative of the velocity potential, ϕ, in the form $d\phi/dx = P\cos(nt+\epsilon)$] for a finite aperture, even of circular form, is probably beyond the power of known

---

* Consultant to GC Optronics, Inc. and Head, Electro-Optical Sci. Ctr., at State Univ. of New York, Stony Brook, N. Y.

[1] D. Gabor, G. W. Stroke, R. Restrick, A. Funkhouser, and D. Brumm, "Optical Image Synthesis (Complex Amplitude Addition and Subtraction) by Holographic Fourier Transformation," Phys. Lett. **18**, 116–118 (1965).

[2] D. Gabor, "A New Microscopic Principle," Nature **161**, 777–778 (1948).

[3] D. Gabor, "Microscopy by Reconstructed Wavefronts," Proc. Roy. Soc. (London) **A197**, 454–487 (1949).

[4] D. Gabor, "Microscopy by Reconstructed Wavefronts, II," Proc. Phys. Soc. (London), **64**, 449–469 (1951).

[5] G. W. Stroke, *An Introduction to Coherent Optics and Holography* (Academic Press Inc., New York, 1966; enlarged ed. March 1969).

[6] J. B. DeVelis and G. O. Reynolds, *Theory and Applications of Holography* (Addison-Wesley Publ. Co., Reading, Mass., 1967).

[7] J. W. Strutt Lord Rayleigh, *The Theory of Sound* (Macmillan and Co., London, 1894), 2nd ed. (revised and enlarged), 2 vols.

methods; . . ." This was indeed still the general case, in most applications, until the recent advent of holographic interferometry.

In this paper, we do not propose to develop further the several applications of holographic interferometry to acoustics, ultrasonics, and, in general, to vibration analysis and theory, which have recently become of new theoretical and experimental interest as a result of the new developments in this field. Rather, we propose to present here, concisely but with the appropriate rigor, the theory of "holographic interferometry," as it has come to be known in recent literature. In a general way, the theory presented herein is based on the theory first published by D. Gabor and G. W. Stroke in 1965, under the title "Optical Image Synthesis (Complex Addition and Subtraction) by Holographic Fourier Transformation."[1] It may be in order to recall that many independent papers on two-beam holographic interferometry appeared starting in 1965 (see, e.g., Refs. 8–14; for a complete list, see references in Ref. 11). Interferometric vibration analysis by wavefront reconstruction was also first described in that year,[11,14] as were related methods for the generation of contour maps of three-dimensional objects by means of holography,[15–17] starting with the two-wavelength method[15] and one[16] that (according to Ref. 17) essentially describes a projection of Young's fringes on the surface of the object (which can be realized by direct observation without the holographic technique). A truly holographic method for the generation of contour maps of diffusely reflecting surfaces using an immersion method was first described in Ref. 17; and early aspects of the problems related to fringe localization, in Refs. 18 and 19, among others.

This and much additional related work has made apparent an increasing need for a unified theory of holographic interferometry. It has now become evident that the foundations for the theory of holographic interferometry were first given in the paper, mentioned above, by Gabor and Stroke.[1] The theoretical development that follows is based on the general principles of that paper and gives a number of new theoretical results that we have obtained in our recent investigations, of which the experimental verifications will be published in a separate part.[20] In the most general way, all contemporary theories and extensions of holography are based on a series of three papers (Refs. 2–4) first published by Gabor between 1948 and 1951. (For a general background on holography, the reader is referred to the appropriate texts.[5,6] As indicated in Ref. 21, more than 500 new papers on holography were listed in 1967 alone; because of the excellence of that classified listing, the reader is referred to that reference for a complete bibliography, in addition to the references given here. References 22–28 are also particularly relevant to this work.)

I. THEORETICAL FOUNDATIONS OF HOLOGRAPHIC INTERFEROMETRY

In a general way, holographic interferometry may be considered as a particular form of "wavefront-reconstruction" imaging, in which two or more images (rather than only one image) of the same object are reconstructed, spatially superimposed, on top of each other, in the same region of space. In cases where the several images are identical and rigorously superimposed on each other, the observer (eye, camera, etc.) sees only one reconstructed "object." However, because of the coherence of the laser light, used both in the recording of the hologram and in the reconstruction of the image, there arises a light-intensity-modulating "interference" between the different reconstructed

[8] J. M. Burch, "The Application of Lasers in Production Engineering," Production Eng. 44, 431–442 (1965).
[9] R. J. Collier, T. E. Doherty, and K. S. Pennington, "Application of Moiré Techniques to Holography," Appl. Phys. Lett. 7, 223–225 (1965).
[10] G. W. Stroke and A. E. Labeyrie, "Two-Beam Interferometry by Successive Recording of Intensities in a Single Hologram," Appl. Phys. Lett. 8, 42–44 (1966).
[11] L. O. Heflinger, R. F. Wuerker, and R. E. Brooks, "Holographic Interferometry," J. Appl. Phys. 37, 642–649 (1966).
[12] J. M. Burch, A. E. Ennos, and R. J. Wilton, "Dual- and Multiple-beam Interferometry by Wavefront Reconstruction," Nature 209, 1015–1016 (1966).
[13] K. A. Stetson and R. L. Powell, "Hologram Interferometry," J. Opt. Soc. Amer. 56, 1161–1166 (1966).
[14] R. L. Powell and K. A. Stetson, "Interferometric Vibration Analysis by Wavefront Reconstruction," J. Opt. Soc. Amer. 55, 1593–1598 (1965).
[15] K. Haines and B. P. Hildebrand, "Contour Generation by Wavefront Reconstruction," Phys. Lett. 19, 10–11 (1965).
[16] B. P. Hildebrand and K. Haines, "The Generation of Three-Dimensional Contour Maps by Wavefront Reconstruction," Phys. Lett. 20, 422–423 (1966); Appl. Opt. 5, 172 (1966).
[17] T. Tsuruta, N. Shiotake, J. Tsujiuchi, and K. Matsuda, "Holographic Generation of Contour Map of Diffusely Reflecting Surface by Using Immersion Method," Jap. J. Appl. Phys. 6, 661–662 (1967).
[18] J. Tsujiuchi and T. Tsuruta, "Holographic Interference Using Rough Surfaces," Jap. J. Appl. Phys. 6, 232–239 (1967).
[19] E. Archibold, J. M. Burch, and A. E. Ennos, "The Application of Holography to the Comparison of Cylinder Bores," J. Sci. Instrum. 44, 489–494 (1967).
[20] G. M. Brown, R. M. Grant, and G. W. Stroke, "The Theory of Holographic Interferometry, II: Experimental Verifications" (unpublished notes).
[21] J. N. Lattia, "A Classified Bibliography on Holography and Related Fields," J. Soc. Motion Picture Television Eng. 77, 1–22 (1968).
[22] G. W. Stroke, "Holography," Sci. Teacher, 34, No. 7, 73–88 (1967).
[23] G. W. Stroke, "Diffraction Gratings," in *Handbuch der Physik*, S. Flügge, Ed. (Springer-Verlag, Berlin, 1967), Vol. 29, pp. 426–754).
[24] R. E. Brooks, L. O. Heflinger, and R. F. Wuerker, "Interferometry with Holographically Reconstructed Comparison Beam," Appl. Phys. Lett. 7, 248–249 (1965).
[25] K. A. Stetson and R. L. Powell, "Interferometric Hologram Evaluation and Real-Time Vibration Analysis of Diffuse Objects," J. Opt. Soc. Amer. 55, 1694–1695 (1965).
[26] D. Gabor, G. W. Stroke, D. Brumm, A. Funkhouser, and A. Labeyrie, "Reconstruction of Phase Objects by Holography," Nature 208, 1159–1162 (1965).
[27] G. W. Stroke and A. E. Labeyrie, "Interferometric Reconstruction of Phase Objects Using Diffuse 'Coding' and Two Holograms," Phys. Lett. 20, 157–158 (1966).
[28] H. Nassenstein, "Holographische Interferometrie Diffus Reflektierender Objekte," Phys. Lett. 21, 290–291 (1966).

images, when these are not exactly superimposed on top of each other.

Similarly, if the original object, of which a singly exposed hologram has been recorded, is observed through the developed hologram replaced into the recording position, then the reconstructed image may be exactly superimposed onto the object (still illuminated in laser light). The light-modulating interference now occurs between the light waves from the actual object, on one hand, as they pass through the hologram, and, on the other, the light waves produced from the hologram by transmission of the laser beam through it. Any relative displacement between the object and the three-dimensional virtual image, superimposed onto it (or any change in the object shape, relative to the reconstructed image, superimposed onto it), will display the object covered by a system of interference fringes, quite similar to the fringes that characterize interferograms obtained with conventional interferometers, using mirrors (for instance of the Michelson–Twyman–Green or Mach–Zehnder types).

In contrast with conventional interferometers, using highly polished mirrors, however, the holographically obtained interferograms display interference fringes also with perfectly diffusing objects. Moreover, because the holographic interferograms measure differences either in shape or in relative displacements, they may be used to study deformations or displacements of objects having dimensions arbitrarily large as compared to the wavelength, even when topological changes of a fraction of a wavelength are being measured. As an example, it is readily possible to measure changes of shape of 1/10 wavelength (equal to only about 600 Å, when the wavelength of 6328 Å of the helium–neon laser is being used), even though the span of the object may be on the order of 1 m (i.e., on the order of 1.5 million wavelengths!).

The mathematical description of holographic interferometry (indeed, of holographic imaging) may perhaps be best understood by first considering the description of the recording and reconstructing processes in terms of "wavefront reconstruction," exactly along the lines first given by Gabor (see also Refs. 5 and 6).

For this purpose, it is first necessary to recall (as shown by O. Wiener in 1890 and by G. Lippmann in 1894 [22]) that photographic emulsions are sensitive to

$$\langle |\tilde{\mathbf{E}}(x,y,z,t)|^2 \rangle$$

(where $\langle\ \rangle$ indicates a time average), when exposed to an electromagnetic field, of which the electric-field-vector component is given by:

$$\tilde{\mathbf{E}}(\mathbf{r},t)=\mathbf{E}(\mathbf{r})\cos\nu t, \tag{1}$$

where $\mathbf{r}(x,y,z)$ is a position vector. Because of the very high frequency of electromagnetic waves at light frequencies (on the order of 5×10^{14} Hz), only time averages are generally observable. We henceforth omit the time factor and deal only with the spatial component:

$$\mathbf{E}(\mathbf{r})=|\mathbf{E}(\mathbf{r})|e^{i\phi(\mathbf{r})}. \tag{2}$$

With reference to Fig. 1, let $\mathbf{E}_O$ be the spatial field produced at some distance from the object when it is illuminated with laser light of some steady-state frequency ν. It is this wave, $\mathbf{E}_O$, which, when focused by the eyes (or a camera), produces an image on the retinas (or photographic emulsion). Significantly, it may be shown that the image-forming information (notably the three-dimensional information) in an unfocused light field, such as $\mathbf{E}_O$, is essentially contained in the phase, $\phi_O(\mathbf{r})$, of the light wave, $\mathbf{E}_O=|\mathbf{E}_O|e^{i\phi_O}$. Accordingly, as first shown by Gabor,[1] any photographic scheme designed to retrievably store the three-dimensional image-forming information con-

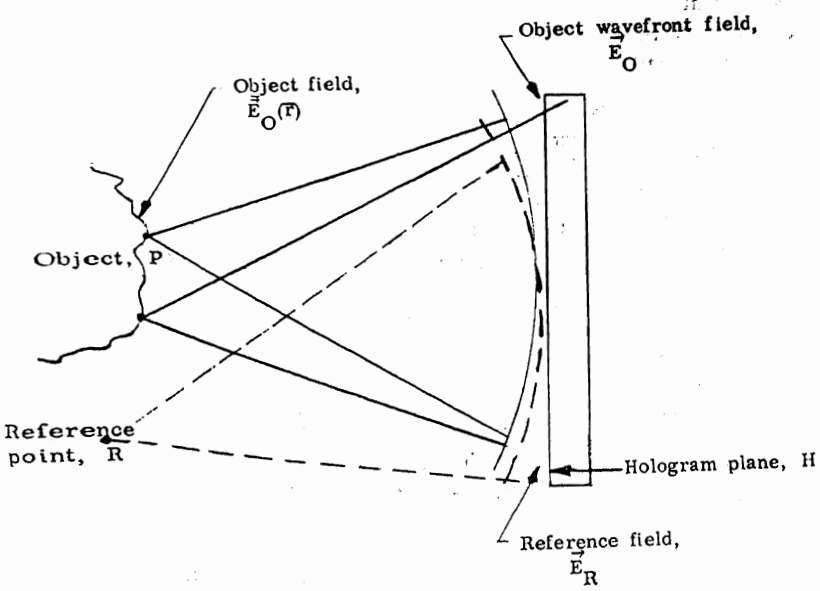

FIG. 1. Method of hologram formation.

tained in $\mathbf{E}_O$ (for the purpose of subsequent release and display of a 3-D image), must necessarily be so designed as to store the phase, ϕ_O, of the wavefront, $\mathbf{E}_O(\mathbf{r})$. The photographic record of the wavefront, $\mathbf{E}_O$, must therefore itself be obtained by making $\mathbf{E}_O$ interfere with some other wave, say $\mathbf{E}_R=|\mathbf{E}_R|e^{i\phi_R}$, commonly called the coherent reference wave or reference background. Indeed, the photographic record of the image-forming wavefront was shown by Gabor to be nothing but a type of wavefront interferogram, which he called a hologram.[2]

The exposure I (commonly, although of course incorrectly, called intensity), in the plane of the photographic emulsion placed as shown in Fig. 1 is given by the equation

$$I=(\mathbf{E}_O+\mathbf{E}_R)(\mathbf{E}_O+\mathbf{E}_R)^* =|\mathbf{E}_O|^2+|\mathbf{E}_R|^2+\mathbf{E}_O\mathbf{E}_R^*+\mathbf{E}_O^*\mathbf{E}_R, \quad (3)$$

where * indicates "the complex conjugate of" (i.e., $\mathbf{E}_O^*=|\mathbf{E}_O|e^{-i\phi_O}$). It may sometimes be useful to write Eq. 3 in the form

$$I=|\mathbf{E}_O|^2+|\mathbf{E}_R|^2+2|\mathbf{E}_O||\mathbf{E}_R|\cos(\phi_O-\phi_R), \quad (4)$$

which displays the diffraction-grating-like nature of holograms, and which also shows that the vector fields, $\mathbf{E}_O$ and $\mathbf{E}_R$, have been recorded in terms of simple intensity (density) variations in the photographic emulsion.[2,3] The purpose of the holographic recording of the wavefront $\mathbf{E}_O$ is to release it subsequently from the hologram. It may be immediately shown with the aid of the theory of holography[5] that the wavefront $\mathbf{E}_O$ may be released from the hologram simply by illuminating the hologram with the reference field $\mathbf{E}_R$, if this field is a simple plane wave (or indeed a spherical wave, if suitable care is used). (For a basic discussion of the principles of holography, see Refs. 5 and 6.) An observer looking at the reconstructed wavefront $\mathbf{E}_O$ will be unable to distinguish between the reconstructed wavefront and the original wavefront $\mathbf{E}_O$ of coherent light scattered by the object.

Because the reconstructed wavefront is identical to the original object wavefront as scattered by the object, one is immediately led to an important and nontrivial conclusion about the spatial-electric fields in the object space and in the reconstructed-image space, respectively. The conclusion is that, regardless of the manner in which the object field is related to the scattered field $\mathbf{E}_O$ used in the recording of the hologram, *reconstruction of the field* $\mathbf{E}_O$, *by means of the hologram, will produce in the reconstructed image a spatial-electric-field-vector distribution identical to the spatial-electric-field-vector distribution in the original object*, under the stated assumptions, and notably provided that the relative positions of the object, reference beam, and hologram are maintained with interferometric precision, as noted above.

An important additional remark about holographic interferometry may be drawn from this conclusion. For the purpose of the subsequent analysis, we may conclude that it is sufficient to know that a given object field $\bar{\mathbf{E}}_O(\mathbf{r})$ produces in the hologram plane a wavefront $\mathbf{E}_O$ and that we may disregard the particular manner in which the object field and the wavefront field are related. Moreover, holographic reconstruction of the wavefront $\mathbf{E}_O$ produces in the reconstructed image a field $\bar{\mathbf{E}}_O(\mathbf{r})$, identical to the original object field, under the stated assumptions.

Henceforth, we describe the object or image fields by

$$\bar{\mathbf{E}}_O(\mathbf{r})=|\bar{\mathbf{E}}_O(\mathbf{r})|e^{i\phi_O(\mathbf{r})},$$

and the corresponding wavefront fields at the hologram plate by

$$\mathbf{E}_O=|\mathbf{E}_O|e^{i\phi_O}.$$

Let us write symbolically

$$\bar{\mathbf{E}}_O\rightarrow\mathbf{E}_O, \quad (5)$$

where Eq. 5 may be interpreted as saying that the object field $\bar{\mathbf{E}}_O$ produces the wavefront field $\mathbf{E}_O$ (in some cases, see e.g. Eq. 6, by a spatial Fourier transformation). We may similarly write symbolically

$$\mathbf{E}_O\rightarrow\bar{\mathbf{E}}_O, \quad (6)$$

where Eq. 6 may be interpreted as saying that the reconstructed wavefront field $\mathbf{E}_O$ reconstructs an image field $\bar{\mathbf{E}}_O$ identical to the object field $\bar{\mathbf{E}}_O$!

Even though Eqs. 5 and 6 are given in purely symbolic form, they may be taken as being particularly helpful in relating the wavefront field to the corresponding object field, from which it originates, or to the corresponding image field, which it reconstructs!

II. DOUBLY EXPOSED HOLOGRAMS AND CORRESPONDING INTERFEROGRAMS

Let us now record two holograms in the same emulsion, and let the recording be carried out *successively* in the same latent image, using a reference wave of the same shape. Let $\bar{\mathbf{E}}_{O1}$ and $\bar{\mathbf{E}}_{O2}$, respectively, describe the object-point fields, for instance, for two different positions or for two different shapes of the object.

Let the first component hologram be

$$I_1=|\mathbf{E}_{O1}|^2+|\mathbf{E}_R|^2+\mathbf{E}_{O1}\mathbf{E}_R^*+\mathbf{E}_{O1}^*\mathbf{E}_R, \quad (7)$$

and let the second component hologram be

$$I_2=|\mathbf{E}_{O2}|^2+|\mathbf{E}_R|^2+\mathbf{E}_{O2}\mathbf{E}_R^*+\mathbf{E}_{O2}^*\mathbf{E}_R. \quad (8)$$

The resultant hologram I is formed by a superposition of the intensities I_1+I_2 of the two component holograms. We have (according to Ref. 1 and especially Ref. 5, pp. 90–96) the equation

$$I=I_1+I_2=|\mathbf{E}_{O1}|^2+|\mathbf{E}_{O2}|^2+2|\mathbf{E}_R|^2 +\mathbf{E}_R^*[\mathbf{E}_{O1}+\mathbf{E}_{O2}]+\mathbf{E}_R[\mathbf{E}_{O1}^*+\mathbf{E}_{O2}^*]. \quad (9)$$

If the hologram I described by Eq. 9, is developed, replaced into its recording position, and illuminated with a simple wave $\mathbf{E}_R$ (identical to the reference wave $\mathbf{E}_R$ used in the recording), it follows immediately from Eq. 9 that the reconstructed wave field will have a term proportional to

$$\mathbf{E}_R\mathbf{E}_R^*[\mathbf{E}_{O1}+\mathbf{E}_{O2}]. \tag{10}$$

Assuming that $\mathbf{E}_R\mathbf{E}_R^*=1$ (which is the case for a plane wave and very closely for a spherical wave), it follows, according to basic theory of holography (Ref. 5, pp. 127–137), that the reconstructed-wavefront field $[\mathbf{E}_{O1}+\mathbf{E}_{O2}]$ produces, in the object domain, an image field

$$\bar{\mathbf{E}}_{O1}+\bar{\mathbf{E}}_{O2}; \tag{11}$$

that is, according to Eq. 6

$$\mathbf{E}_{O1}+\mathbf{E}_{O2}\rightarrow\bar{\mathbf{E}}_{O1}+\bar{\mathbf{E}}_{O2}. \tag{12}$$

The reconstructed-image field, described by Eq. 11, describes the field *at each point* of the reconstructed-image field (in the object domain). The resultant field vector at each point in the reconstructed-image field may be written explicitly as

$$\bar{\mathbf{E}}_{\text{image}}(\mathbf{r})=\bar{\mathbf{E}}_{O1}(\mathbf{r})+\bar{\mathbf{E}}_{O2}(\mathbf{r}+\Delta\mathbf{r}). \tag{13}$$

Because the displacements, or deformations, considered in holographic interferometry are generally very small compared to the coordinates, x, y, z, of the object relative to the hologram, one may conclude that the image-field vector in the reconstructed image $\bar{\mathbf{E}}_{\text{image}}$ is given, at each point, simply by the vector sum of the corresponding fields reconstructed in the two superimposed images, as given by $\bar{\mathbf{E}}_{O1}$ and $\bar{\mathbf{E}}_{O2}$ and projected onto the same point $(\mathbf{r})$. (The applicability of Eq. 13 and of related equations applicable to the case of vibrating objects, "real-time" interferometry, and so on, is more completely discussed in Sec. III.)

Under these conditions, we may write

$$|\bar{\mathbf{E}}_{O1}|\cong|\bar{\mathbf{E}}_{O2}|=|\bar{\mathbf{E}}_O|, \tag{14}$$

with

$$\bar{\mathbf{E}}_{O1}=|\bar{\mathbf{E}}_O|\,e^{i\phi_{O1}} \tag{15}$$

and

$$\bar{\mathbf{E}}_{O2}=|\bar{\mathbf{E}}_O|\,e^{i\phi_{O2}}. \tag{16}$$

The intensity distribution in the reconstructed image, corresponding to Eq. 13, is thus

$$I_{\text{image}}=2|\mathbf{E}_O|^2[1+\cos(\phi_{O2}-\phi_{O1})], \tag{17}$$

where $(\phi_{O2}-\phi_{O1})$ is a direct measure of the displacement

$$\Delta\mathbf{r}=\Delta\mathbf{x}+\Delta\mathbf{y}+\Delta\mathbf{z}, \tag{18}$$

projected into the directions of illumination $\mathbf{n}_1$ and of observation, $\mathbf{n}_2$, respectively. We may immediately write (for further details see Sec. V)

$$\phi_{O2}-\phi_{O1}=(2\pi/\lambda)\Delta\mathbf{r}\cdot(\mathbf{n}_1+\mathbf{n}_2). \tag{19}$$

Equation 17 describes the "contour-map" interferogram obtained by double-exposure holography. With Eq. 19, we thus recognize that the interferograms obtained by double-exposure holography (even of diffusely scattering objects!) are indeed identical to interferograms that would be obtained, if classical two-beam interferometry[10] could produce interferograms of diffusely scattering objects.

In summary, we may also state that successive summation of *intensities* in the holographic plate produces, by holographic image reconstruction, in the object domain, a field-vector summation, at the respective object points, identical to that which would have been obtained if the two object fields had in fact existed *simultaneously*!

III. MULTIPLY EXPOSED HOLOGRAMS (CASE OF MOVING OR VIBRATING OBJECTS) AND CORRESPONDING INTERFEROGRAMS

When we record a hologram of a moving or vibrating object by making the wavefronts scattered by the object interfere with a steady coherent background, we find, in practice, that the resulting hologram consists of a superposition of the *intensities* of a great number of component holograms, one for each "instantaneous" position of the object, as it moves (say, for instance, back and forth) relative to the hologram. The superposition of intensities is a consequence of the fact that most velocities of motion or of vibration encountered in practice are sufficiently small, as compared to the velocity of light ($c=3\times10^8$ m/sec), so that a "snapshot" component hologram of the type described by Eqs. 7, 8, and so forth, is recorded for each "instantaneous" steady position, in differential increments. (This conclusion may be shown to be consistent with a relativistic analysis and the corresponding Doppler shifts in the scattered laser light.)

It follows immediately, from the preceding consideration and from the analysis in Sec. II, that *when a hologram is recorded by interference between a reference field* $\mathbf{E}_R$ on one hand and, on the other, a *set of scattered wavefront fields* $\mathbf{E}_{O,l=1,2,3\ldots}$, each corresponding to a successive position (or shape) of the object, at given times t, so that each point on the object may be described by a vector $\mathbf{r}$ at the time t and the corresponding field, at each object point, by $\bar{\mathbf{E}}_O(\mathbf{r},t)$, then this hologram will simultaneously reconstruct, at each object point in the reconstructed-image field, the superposition of all these electric-field values, each properly weighted by the total fractional duration of the total exposure time that was occupied by any of the component object-point-field values $\bar{\mathbf{E}}_O(\mathbf{r},t)$ as if all these field values had in fact existed simultaneously.

In simple words, we may say that *a multiply exposed hologram of a moving or of a vibrating object reconstructs an image, in which the reconstructed image-field vector, at each object point, is equal to the time average of the*

object-field-vector values taken on by the particular object point during the course of the photographic exposure.

Indeed, let

$$\bar{\mathbf{E}}_{O1}(\mathbf{r}_1,t_1)$$

be the object-point-field value (relative to the steady reference beam $\mathbf{E}_R$ and fixed hologram), and let this field value last for a duration Δt_1 that is for a fraction

$$\Delta t_1/T$$

of the total exposure time T. According to the theory first given by Gabor and Stroke, *et al.*,[1] and in conformity with Sec. II, we know that the corresponding image-point-field value, reconstructed from the "superposition hologram" in the object space, will be

$$\bar{\mathbf{E}}_{\text{image}}(\mathbf{r}_1)=\bar{\mathbf{E}}_{O1}(\mathbf{r}_1,t_1)\Delta t_1/T. \tag{20}$$

Similarly we shall have, in general, for the general object-point-field value $\bar{\mathbf{E}}_O(\mathbf{r},t)$ lasting a fraction $\Delta t/T$ during the exposure, in the image field, the value

$$\mathbf{E}_{\text{image}}(\mathbf{r})=\bar{\mathbf{E}}_O(\mathbf{r},t)\Delta t/T, \tag{21}$$

and the total resulting value of the field in the image, at any image point, is equal (in the limit) to

$$\bar{\mathbf{E}}_{\text{image}}(\mathbf{r})=\frac{1}{T}\int_0^T \bar{\mathbf{E}}_O(\mathbf{r},t)dt. \tag{22}$$

Before proceeding to clarify Eq. 22 further with the aid of specific examples and for the case of some geometrical situations of major interest, it may be in order to first indicate that Eq. 22 may, in general, be simplified, when the component object-point fields may be considered to be of the form

$$\bar{\mathbf{E}}_O(\mathbf{r},t)=\bar{\mathbf{E}}_O(\mathbf{r})e^{i\phi_O(\mathbf{r},t)}; \tag{23}$$

that is to say, when it is possible to consider that only the local spatial phase of the object point (relative to the hologram and to $\mathbf{E}_R$) varies with time. This case, of great practical importance in interferometry, also results in appreciable mathematical simplification, for instance in such cases as are considered in what follows. Under the assumptions of Eq. 23, we may write Eq. 22 in the form

$$\bar{\mathbf{E}}_{\text{image}}(\mathbf{r})=\bar{\mathbf{E}}_O(\mathbf{r})\frac{1}{T}\int_0^T e^{i\phi_O(\mathbf{r},t)}dt, \tag{24}$$

where $\bar{\mathbf{E}}_O(\mathbf{r})$ describes the object-point-field value at the point $\mathbf{r}$ as it would be reconstructed from a simple, two-beam hologram, such as that of Eq. 13. Equation 24 has considerable importance, in that it shows that the multiply exposed (superpositioned) hologram reconstructs an image that is identical to the image of the static (nonmoving) object, except that the field value, at each point $\mathbf{r}$ in the reconstructed image, is modulated by the time average of the phase values $\phi_O(\mathbf{r},t)$ corresponding to the distance values of the moving object point, relative to the hologram and to $\mathbf{E}_R$. We may recall that, in general, the phase ϕ is related to an optical-path difference Δ by the equation

$$\phi=(2\pi/\lambda)\Delta, \tag{25}$$

where λ is the wavelength of the light radiation.

We may also recall, for completeness, that the final image, as seen by the eye or photographed by a camera, displays

$$|\bar{\mathbf{E}}_{\text{image}}(\mathbf{r})|^2=|\bar{\mathbf{E}}_O(\mathbf{r})|^2\left|\left[\frac{1}{T}\int_0^T e^{i\phi_O(\mathbf{r},t)}dt\right]\right|^2. \tag{26}$$

As a result, the three-dimensional image of the object will again appear "covered" by a "contour-map" system of interference fringes.

Before deriving a general expression giving d and therefore ϕ and the corresponding fringe system in terms of the holographic recording layout and the motion of the object, it appears useful to first consider a number of simple cases.

IV. PLANE-VIBRATING MIRROR, ILLUMINATED AND OBSERVED NORMALLY TO ITS SURFACE

Let a plane mirror M be vibrating with an amplitude m at a circular frequency ω as shown in Fig. 2. We may write

$$d=m\sin\omega t, \tag{27}$$

where d describes, in this case, the change of distance of the mirror relative to a reference plane, which we take to be the hologram plane. To determine the corresponding path difference Δ, it is necessary to consider the entire holographic interferometer, which may be most readily modeled in the form of a Michelson-Twyman-Green arrangement, as shown in Fig. 3.

It is clear from Fig. 3 that the path-difference change Δ corresponding to a distance change d is

$$\Delta=2d \tag{28}$$

for the model used.

The corresponding phase change is

$$\phi=(2\pi/\lambda)\Delta. \tag{29}$$

It follows that the instantaneous object-point-field value at the point $\mathbf{r}$ is given by

$$\bar{\mathbf{E}}_O(\mathbf{r},t)=\bar{\mathbf{E}}_O(\mathbf{r})e^{i(2\pi/\lambda)2m\sin\omega t}. \tag{30}$$

We then immediately find, according to Eq. 24, that the field values of the vibrating object, in the image reconstructed from the superpositioned hologram, are given by the equation

$$\bar{\mathbf{E}}_{\text{image}}(\mathbf{r})=\bar{\mathbf{E}}_O(\mathbf{r})\frac{1}{T}\int_0^T e^{i(2\pi/\lambda)2m\sin\omega t}dt. \tag{31}$$

Before further developing Eq. 31, it is of interest to examine the general case, as given in the next Section.

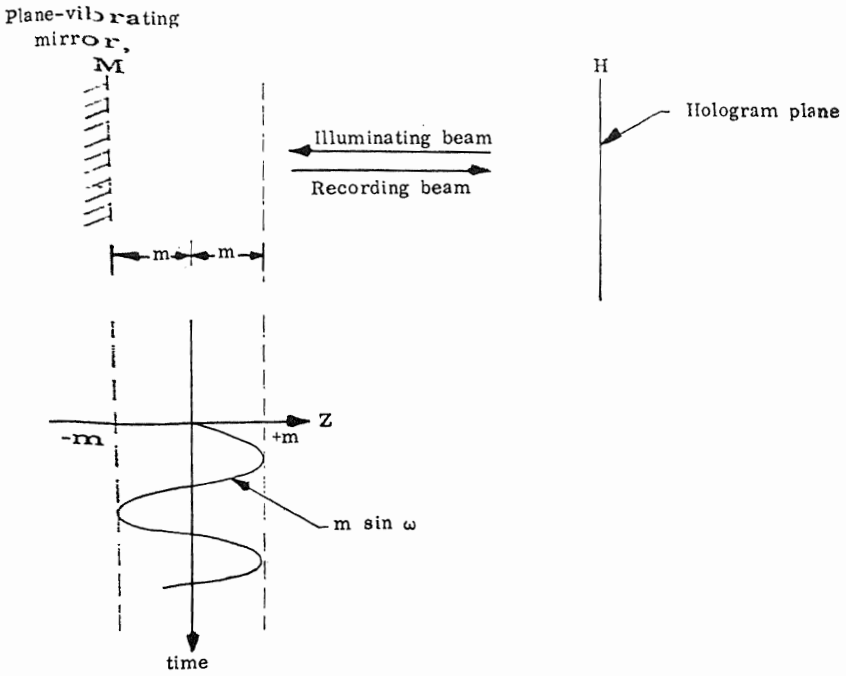

FIG. 2. Geometry for plane-vibrating mirror, illuminated and observed normally to its surface.

V. CASE OF SINUSOIDALLY VIBRATING OBJECT WITH OBLIQUE ILLUMINATION AND WITH OBLIQUE RECORDING DIRECTION, RELATIVE TO THE OBJECT

Let us consider the holographic interferometry arrangement as modeled in Fig. 4. Let us assume, first, that we use the same direction for the reference beam in the recording and for the observation in the reconstruction, and let us describe the corresponding direction by the unit vector $\mathbf{n}_1$. Let us further assume that the direction of vibration of a point $P(\mathbf{r})$ on the surface of the vibrating object may be described by the unit vector $\mathbf{n}_m$. By considering the geometry of Fig. 5, we now find that we may write the phase component of the point $P(\mathbf{r})$ in the direction $\mathbf{n}_1$ in the form

$$(\mathbf{n}_1\cdot\mathbf{n}_m)(2\pi/\lambda)2m\sin\omega t, \tag{32}$$

where the dot between $\mathbf{n}_1$ and $\mathbf{n}_m$ indicates a vector dot product. This may be readily seen, in Fig. 5, by noting that the projection of $2m$ from the direction $\mathbf{n}_m$ onto the direction $\mathbf{n}_1$ is equal to $2m\cos\theta_1$, i.e., is equal to

$$2m(\mathbf{n}_1\cdot\mathbf{n}_m), \tag{33}$$

where θ_1 is the angle between $\mathbf{n}_1$ and $\mathbf{n}_m$.

In general, it is conceivable to have not only an illumination of the vibrating (or moving) object along a direction $\mathbf{n}_1$ but also a direction of recording $\mathbf{n}_2$ different from $\mathbf{n}_1$ (see Fig. 6). If we now call θ_1 the angle between $\mathbf{n}_1$ and $\mathbf{n}_m$ and θ_2 the angle between $\mathbf{n}_2$ and $\mathbf{n}_m$, and if we again assume "small" angles θ_1 and θ_2 (or correspondingly small local slopes in the surface of the object), we find (Fig. 6) that the path difference

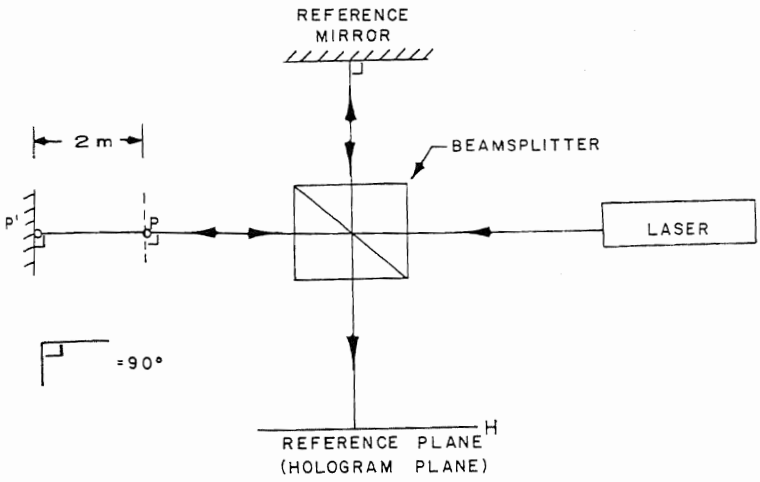

FIG. 3. Holographic interferometer model (normal illumination and recording direction).

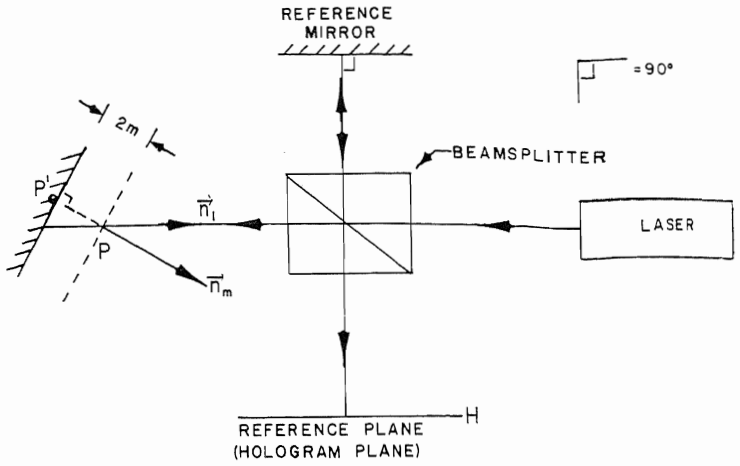

FIG. 4. Holographic interferometer model (oblique illumination and recording direction).

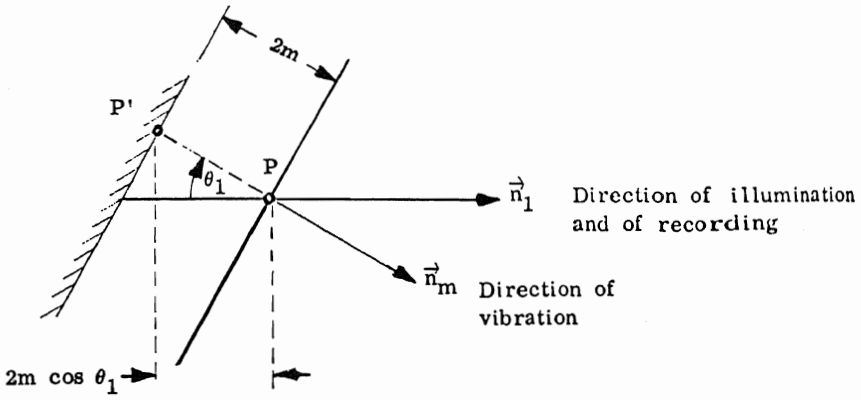

FIG. 5. Geometry for oblique, colinear illumination and recording of plane-vibrating mirror.

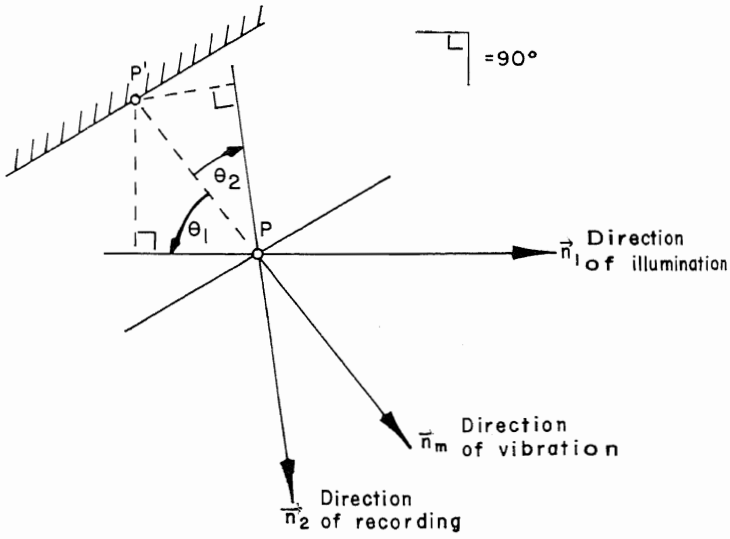

FIG. 6. Geometry for general case of oblique illumination and recording of plane-vibrating mirror.

Δ corresponding to this situation is now given by

$$\Delta = m\mathbf{n}_m \cdot (\mathbf{n}_1 + \mathbf{n}_2), \tag{34}$$

as may be readily verified by noting that the "ingoing" increase in distance is

$$d_{\text{in}} = m\mathbf{n}_m \cdot \mathbf{n}_1, \tag{35}$$

that the "outgoing" increase in distance is

$$d_{\text{out}} = m\mathbf{n}_m \cdot \mathbf{n}_2, \tag{36}$$

and that the corresponding path difference is

$$\Delta = d_{\text{in}} + d_{\text{out}}. \tag{37}$$

We may now immediately give the general equation, which describes the holographically reconstructed image field in the form

$$\bar{\mathbf{E}}(\mathbf{r})_{\text{image}}=\bar{\mathbf{E}}_O(\mathbf{r})\frac{1}{T}\int_0^T e^{i(2\pi/\lambda)m\mathbf{n}_m\cdot(\mathbf{n}_1+\mathbf{n}_2)\sin\omega t}dt. \quad (38)$$

The corresponding intensity in the image, as observed by the eye (or recorded by a photographic camera), is given by the equation

$$I(\mathbf{r})_{\text{image}}=|\bar{\mathbf{E}}(\mathbf{r})_{\text{image}}|^2 \times\left|\frac{1}{T}\int_0^T e^{i(2\pi/\lambda)m\mathbf{n}_m\cdot(\mathbf{n}_1+\mathbf{n}_2)\sin\omega t}dt\right|^2, \quad (39)$$

that is,

$$I(\mathbf{r})_{\text{image}}=I_O(\mathbf{r}) \times\left[\left|\frac{1}{T}\int_0^T e^{i(2\pi/\lambda)m\mathbf{n}_m\cdot(\mathbf{n}_1+\mathbf{n}_2)\sin\omega t}dt\right|\right]^2, \quad (40)$$

where we have written for the intensity in the holographic image of a static object the expression

$$I_O(\mathbf{r})=|\mathbf{E}_O(\mathbf{r})|^2 \quad (41)$$

under the previously stated assumptions.

Before concluding this Section, we show that the sinusoidal nature of the vibration permits one to simplify the preceding equations further. Indeed, we may write Eq. 38 in the form

$$\bar{\mathbf{E}}(\mathbf{r})_{\text{image}}=\bar{\mathbf{E}}_O(\mathbf{r})\frac{1}{T}\int_0^T e^{iZ\sin\psi}dt \quad (42)$$

where

$$Z=(2\pi/\lambda)m\mathbf{n}_m\cdot(\mathbf{n}_1+\mathbf{n}_2),$$

and

$$\psi=\omega t. \quad (43)$$

We may now use well-known identity (Ref. 23, p. 548, and Ref. 29)

$$e^{iZ\sin\psi}\equiv J_0(Z)+\sum_{n=1}^{\infty}J_{2n}(Z)\cos 2n\psi +\sum_{n=0}^{\infty}J_{2n+1}(Z)\sin(2n+1)\psi, \quad (44)$$

where the J's are Bessel functions of integral order.

Equation 42 is considerably simplified when the exposure time T is very large as compared to the period of vibration $(1/\omega)$. We may describe the situation in the limit when $T\to\infty$. Indeed, let us examine the separate parts of the integral

$$\frac{1}{T}\int_0^T e^{iZ\sin\omega t}dt$$

in the limit when $T\to\infty$. We readily find that all integrals, except that with the zero-order Bessel function, tend to zero. Indeed, we have

$$\lim_{T\to\infty}\frac{1}{T}\int_0^T J_0(Z)dt=J_0(Z), \quad (45)$$

but

$$\lim_{T\to\infty}\frac{1}{T}\int_0^T J_{2n}(Z)\cos 2n\omega t dt =\lim_{T\to\infty}\frac{1}{T}\int_0^T J_{2n}(Z)\frac{1}{2n\omega}[\sin 2n\omega t]_0^T=0, \quad (46)$$

and

$$\lim_{T\to\infty}\frac{1}{T}\int_0^T J_{2n+1}(Z)\sin 2n\omega t dt=0. \quad (47)$$

Accordingly, we find, in the limit of exposure times T that are long as compared to the vibration period, that the field values in the image reconstructed from a "time-average" hologram may be written in the form

$$\bar{\mathbf{E}}(\mathbf{r})_{\text{image}}=\bar{\mathbf{E}}_O(\mathbf{r})J_0[(2\pi/\lambda)m\mathbf{n}_m\cdot(\mathbf{n}_1+\mathbf{n}_2)]. \quad (48)$$

The intensity in the image holographically reconstructed from a multiply exposed (time-averaged) hologram of a vibrating object is thus simply given by the equation

$$I(\mathbf{r})_{\text{image}}=I_O(\mathbf{r})|J_0[(2\pi/\lambda)m\mathbf{n}_m\cdot(\mathbf{n}_1+\mathbf{n}_2)]|^2. \quad (49)$$

Because Eq. 49 has come to have such a considerable practical importance, it deserves some further discussion.

First of all, Eq. 49 describes the interference fringe system that "covers" the image of the object, under the stated assumptions, in the form of a "contour map" notably in the case where the *same* vectors $\mathbf{n}_m$, $\mathbf{n}_1$, and $\mathbf{n}_2$ are applicable to *all points* (of interest) of the vibrating object. In practice, it may be necessary to take certain precautions in the arrangement of the holographic interferometer to satisfy this condition. We shall return to this point and to the related point of "fringe localization" below. It may suffice to state here that the "sameness" condition for the vectors, $\mathbf{n}_m$, $\mathbf{n}_1$, and $\mathbf{n}_2$, may be readily achieved with the aid of a "telecentric" arrangement, such as that illustrated in Fig. 7. Significantly, as a result of the two-step nature of holographic imaging, the telecentric (plane-wave illumination and observation) conditions may be achieved in part in the recording and in part during the reconstruction. As an example, we see from Fig. 7 that the condition for "sameness" for $\mathbf{n}_1$ and $\mathbf{n}_2$, respectively, may be met by assuring the "sameness" of $\mathbf{n}_1$ for all

[29] J. A. Stratton, *Electromagnetic Theory* (McGraw-Hill Book Co., New York, 1941), p. 440.

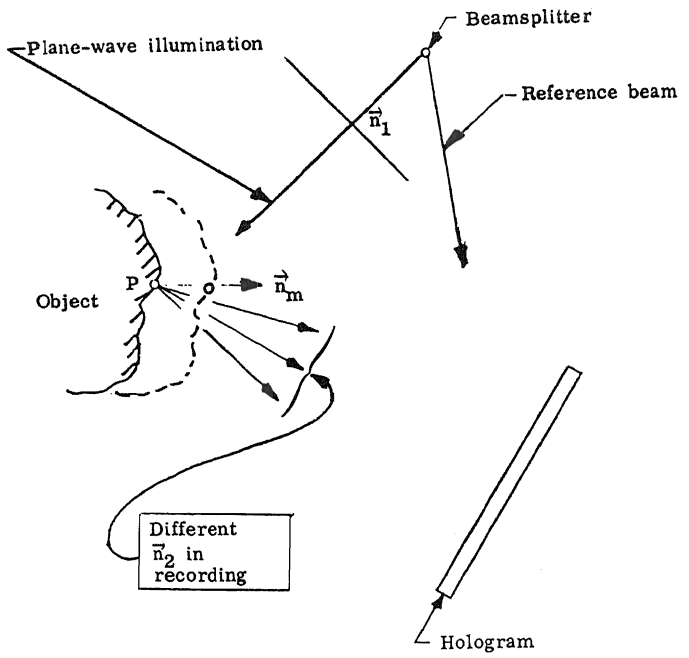

(a) Recording

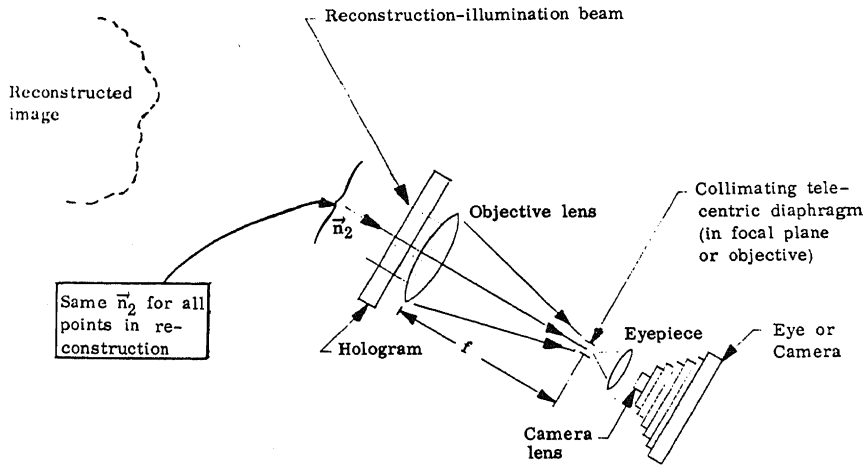

(b) Reconstruction

FIG. 7. Method for assuring "sameness" of $\mathbf{n}_1$ and $\mathbf{n}_2$ for all object points in holographic interferometry.

object points, with the help of plane-wave illumination in the recording of the hologram, and by materializing the "sameness" of $\mathbf{n}_2$ for all points of the object, with the aid of a "telecentric" observation system in the reconstruction.

Equation 49 may also be written in the form

$$I(\mathbf{r})_{\text{image}}=I_O(\mathbf{r})\,|J_0[(2\pi/\lambda)m(\cos\theta_1+\cos\theta_2)]|^2, \quad (50)$$

in which θ_1 and θ_2, respectively, indicate the angle of the motion vector $\mathbf{n}_m$ with the direction of illumination $\mathbf{n}_1$ and of observation $\mathbf{n}_2$, respectively.

Equations 49 and 50 describe the locus of the system of interference fringes that "cover" the object when its image is reconstructed from the "time-average" hologram. The significant parameter is the argument of the J_0 Bessel function, that is,

$$[(2\pi/\lambda)m(\cos\theta_1+\cos\theta_2)]. \quad (51)$$

We may call the function

$$|J_0[(2\pi/\lambda)m(\cos\theta_1+\theta_2]|^2 \quad (52)$$

the "characteristic function" for time-average holography.

Figure 8 graphically represents the characteristic function, and Table I gives numerical values for the "zeros" of the characteristic function.

We may first note that the characteristic function

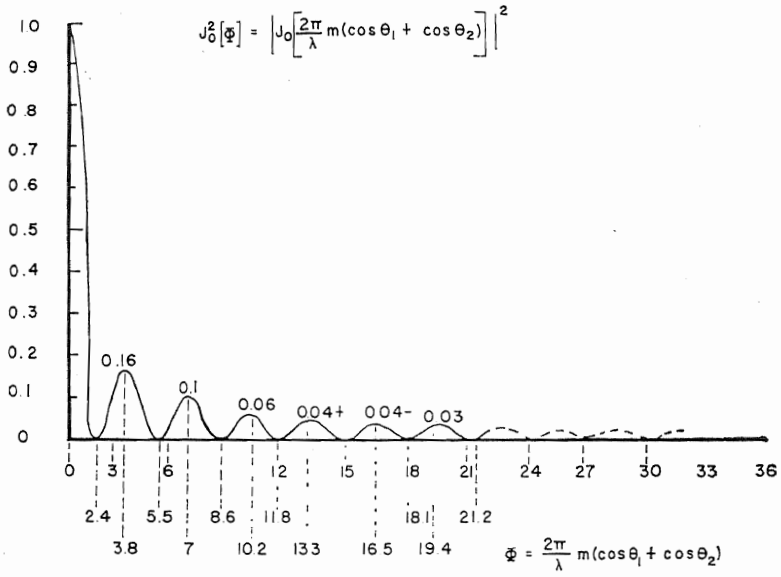

FIG. 8. Plot of the square of the zero-order Bessel function.

is maximum (equal to 1) for the case when

$$m=0, \tag{53}$$

that is, for the parts of the object that remain undisplaced throughout the entire recording time. (We may also note, parenthetically, that the argument of the characteristic function would also be zero for the case

$$\theta_1=\theta_2=\pi/2, \tag{54}$$

that is, when both the illumination and the observation directions would be strictly "orthogonal" to the motion vector, $\mathbf{n}_m$.)

We next note that the reconstructed object will appear to be dark in all regions where the Bessel function J_0 is zero, according to the values given in Fig. 8 and in Table I.

Let us describe the argument of the characteristic function by Φ; that is, let us write Eq. 51 in the form

$$[(2\pi/\lambda)m(\cos\theta_1+\cos\theta_2)]=\Phi. \tag{55}$$

It may be readily seen from the graph of:

$$|J_0[(2\pi/\lambda)m(\cos\theta_1+\cos\theta_2)]|^2$$

in Fig. 8 (and from Table I) that the "zeros" of the characteristic function, i.e., the values

$$\Phi_{0n} \quad (n=1, 2, 3, \cdots), \tag{56}$$

describe the following amplitudes of motion:

$$m_n=(\lambda/2\pi)[1/(\cos\theta_1+\cos\theta_2)]\Phi_{0n}. \tag{57}$$

For instance, in case where the motion vector $\mathbf{n}_m$ is in the direction of illumination and of observation, the zeros of the characteristic function correspond to amplitudes of motion given by

$$m_n=\frac{\lambda}{2\pi}\tfrac{1}{2}\Phi_{0n}. \tag{58}$$

Thus, the first zero, $\Phi_{01}=2.4$, corresponds to an amplitude m_1 of the sinusoidal motion approximately equal to

$$m_1=\frac{\lambda/2}{2\pi}2.4$$

$$\cong 0.383\lambda/2$$

$$\cong 0.19\lambda.$$

All portions of the object moving with this amplitude will be covered with a dark "fringe," and this will be the *first* fringe adjoining the brightest region of the image (for which there is no motion, and for which the argument of the characteristic function is zero).

The second dark interference fringe corresponds to the locus of points, for which the amplitude of motion is given by

$$m_2=\frac{\lambda/2}{2\pi}\Phi_{02}$$

$$\cong\frac{\lambda/2}{2\pi}5.52$$

$$\cong 0.443\lambda,$$

and so on.

In brief, we may conclude this discussion by the following statement. Time-average holography permits one to reconstruct an image of a vibrating object, in which the object appears covered with a system of interference fringes, such that each fringe describes the locus of points vibrating with the same amplitude,

TABLE I. Fringe values, Δ_n and $\Delta_n/2$, at dark fringe number n for time-average holography. Values of the amplitude m_n for normal illumination and observation.[a]

Dark fringe number n	Value of nth zero of $J_0^2(\Phi_{0n})=0$ Φ_{0n}	$\Delta_n=(\lambda/2\pi)\Phi_{0n}$ (μin.)	$m_n=\Delta_n/2$ (μin.)
1	2.405	9.536	4.768
2	5.520	21.89	10.94
3	8.634	34.24	17.12
4	11.79	46.75	23.37
5	14.93	59.20	29.60
6	18.07	71.66	35.82
7	21.21	84.11	42.06
8	24.35	96.57	48.29
9	27.49	109.0	54.51
10	30.64	121.5	60.74
11	33.78	133.9	66.97
12	36.92	146.4	73.20
13	40.06	158.9	79.43
14	43.20	171.3	85.66
15	46.34	183.8	91.89
16	49.48	196.2	98.11
17	52.62	208.7	104.3
18	55.77	221.1	110.6
19	58.91	233.6	116.8
20	62.05	246.1	123.0
21	65.19	258.5	129.3
22	68.33	271.0	135.5
23	71.47	283.4	141.7
24	74.61	295.9	147.9
25	77.76	308.3	154.2
26	80.90	320.8	160.4
27	84.04	333.2	166.6
28	87.18	345.7	172.9
29	90.32	358.2	179.1
30	93.46	370.6	185.3
31	96.61	383.1	191.5
32	99.75	395.5	197.8
33	102.89	408.0	204.0
34	106.0	420.5	210.2
35	109.2	432.9	216.5
36	112.3	445.4	222.7
37	115.5	457.8	228.9
38	118.6	470.3	235.1
39	121.7	482.7	241.4
40	124.9	495.2	247.6

[a] $\lambda=0.6328\ \mu=24.914\ \mu$in., $\Phi_{0n}=(2\pi/\lambda)m_n(\cos\theta_1+\cos\theta_2)$, $\Delta_n=(\lambda/2\pi)\Phi_{0n}=m_n(\cos\theta_1+\cos\theta_2)$, $m_n=\Delta_n/(\cos\theta_1+\cos\theta_2)$.

m_n, where successively increasing amplitudes are given by the equation

$$m_n=(\lambda/2\pi)[1/(\cos\theta_1+\cos\theta_2)]\Phi_{0n}$$

(where Φ_{0n} are the successive zeros of the Bessel function of order zero, J_0). The successively increasing amplitudes of vibration are to be taken starting from all those points (or regions) on the object for which the amplitude of vibration is zero (and which appear to be the brightest in the image). (In cases when there exists no region of the object having "zero" motion, the graph of Fig. 8 may still be used to determine the amplitudes of motion. It is readily seen that the intensity of the reconstructed image in the bright regions as well as in the dark regions may be read from the same graph. In fact, the maxima of the $|J_0|^2$ curve may be taken as describing the locus of the points vibrating with the corresponding amplitudes. Since the first "secondary" maximum is seen to have a relative intensity of 0.16, as compared to unity, corresponding to a complete absence of vibration, the absence of a region with "zero" motion may quite readily be detected by mere inspection of the reconstructed image. If necessary, a nonvibrating object may be readily placed into the field, for reference.)

VI. CASE OF AN OBJECT MOVING WITH LINEAR MOTION COMPONENTS

Because of the general complexity of the motion components that may be possible for an object under study in holographic interferometry, we may consider the form taken on by Eqs. 24 and 26 for those points of the object of which the displacement vector is a linear function of time.

If we describe the position of any point P on the object by $\mathbf{r}$, and if we describe by $\mathbf{m}(\mathbf{r},t)$ the motion of the point during the recording time T of the hologram, as heretofore, then we may consider the particular case of motions for which the velocity $\mathbf{v}(\mathbf{r})$ is uniform (of constant magnitude and direction), such that

$$(d/dt)\mathbf{m}(\mathbf{r},t)=\mathbf{v}(\mathbf{r}), \tag{59}$$

with

$$\mathbf{v}(\mathbf{r})=\mathbf{n}_v v. \tag{60}$$

The displacement of the point $P(\mathbf{r})$ at the time t is then given by

$$\mathbf{m}(\mathbf{r},t)=\mathbf{v}(\mathbf{r})t. \tag{61}$$

Equation 24 may now be written, for each object point in the form

$$\mathbf{E}_{\text{image}}(\mathbf{r})=\mathbf{E}_O(\mathbf{r})\frac{1}{T}\int_0^T e^{i(2\pi/\lambda)\mathbf{v}(\mathbf{r})t\cdot(\mathbf{n}_1+\mathbf{n}_2)}dt. \tag{62}$$

By integration, we immediately obtain the equation

$$\mathbf{E}_{\text{image}}(\mathbf{r})=\mathbf{E}_O(\mathbf{r})\times\left\{\frac{\exp[i(2\pi/\lambda)\mathbf{v}(\mathbf{r})T\cdot(\mathbf{n}_1+\mathbf{n}_2)]-1}{i(2\pi/\lambda)\mathbf{v}(\mathbf{r})T\cdot(\mathbf{n}_1+\mathbf{n}_2)}\right\}. \tag{63}$$

The corresponding intensity at each point in the image is given, according to Eq. 26, by the expression

$$I_{\text{image}}(\mathbf{r})=|\mathbf{E}_{\text{image}}(\mathbf{r})|^2=|\mathbf{E}_O(\mathbf{r})|^2\times\left[\frac{2-2\cos[(2\pi/\lambda)\mathbf{v}(\mathbf{r})T\cdot(\mathbf{n}_1+\mathbf{n}_2)]}{[(2\pi/\lambda)\mathbf{v}(\mathbf{r})T\cdot(\mathbf{n}_1+\mathbf{n}_2)]^2}\right], \tag{64}$$

that is, by

$$I_{\text{image}}(\mathbf{r})=|\mathbf{E}_O(\mathbf{r})|^2\frac{\sin^2\frac{1}{2}[(2\pi/\lambda)\mathbf{v}(\mathbf{r})T\cdot(\mathbf{n}_1+\mathbf{n}_2)]}{\frac{1}{2}[(2\pi/\lambda)\mathbf{v}(\mathbf{r})T\cdot(\mathbf{n}_1+\mathbf{n}_2)]}, \tag{65}$$

which may be written in the form

$$I_{\text{image}}(\mathbf{r})=I_O(\mathbf{r})\ \text{sinc}^2\tfrac{1}{2}[(2\pi/\lambda)\mathbf{v}(\mathbf{r})T\cdot(\mathbf{n}_1+\mathbf{n}_2)]. \tag{66}$$

The conclusion described in Eqs. 65 and 66 is rather remarkable. We find that points of the object moving

with a uniform velocity are indeed reconstructed darker than the points of the object that have not moved during the recording time, T, up to a distance such that the argument

$$\tfrac{1}{2}[(2\pi/\lambda)\mathbf{v}(\mathbf{r})T\cdot(\mathbf{n}_1+\mathbf{n}_2)]$$

of the sinc² becomes equal to π. That is to say that the image reconstructs "black" for values of vT given by the equation

$$\tfrac{1}{2}[(2\pi/\lambda)vT\mathbf{n}_v\cdot(\mathbf{n}_1+\mathbf{n}_2)]=n\pi, \quad n=1, 2, 3, \cdots. \quad (67)$$

For instance, for the case of the illumination and the observation vectors parallel to the velocity unit vector $\mathbf{n}_v$, we have the equation:

$$vT=\lambda/2, \quad (68)$$

showing that a total object displacement of $\lambda/2$ (at uniform velocity) during the recording time results in a total disappearance ("blackening") of the image.

Remarkable as the above conclusion may be, notably for holography in general, we further note that the sinc² function does not remain completely zero, following this first minimum. Indeed, as may be seen from Fig. 9, secondary maxima (albeit very weak ones, compared to the "no-motion" value of 1.0), with the values 0.045 (4.5%), 0.0162 (1.62%), etc., appear for displacements of $3\lambda/4$, $5\lambda/4$, etc.

An additional conclusion may be drawn from the preceding analysis. Equation 66 may be used to determine the maximum allowable velocity of motion in pulsed-laser holography with moving objects.

Indeed, let us assume that adequate imaging may still be obtained with a value of sinc² equal to 0.5 (see Fig. 9), which corresponds approximately to a displacement of $\lambda/4$ at a uniform velocity v in the time T, during which the hologram is being recorded.

As an example, let us say that the hologram is being recorded with a pulsed laser in 100 nsec ($10^2\times10^{-9}$ sec). The allowable velocity is

$$v=\frac{\lambda/4}{T}=\frac{\lambda/4}{10^{-7}}\ \text{sec}^{-1},$$

$$\lambda=6.3\times10^3\times10^{-10}\ \text{m}$$

$$=6.3\times10^{-7}\ \text{m},$$

and

$$v\cong6.3/4=1.6\ \text{m/sec}.$$

In a somewhat more general way, we may say that the maximum allowable (linear) velocity of the component of motion of the object toward the hologram, for good holographic imaging, is on the order of

$$v_{\max}\leq\frac{\lambda/5}{T}, \quad (69)$$

where T is the duration of the recording of the hologram! For "perfect" imaging, the tolerance may be even smaller, say on the order of

$$v_{\max}\leq\frac{\lambda/15}{T}.$$

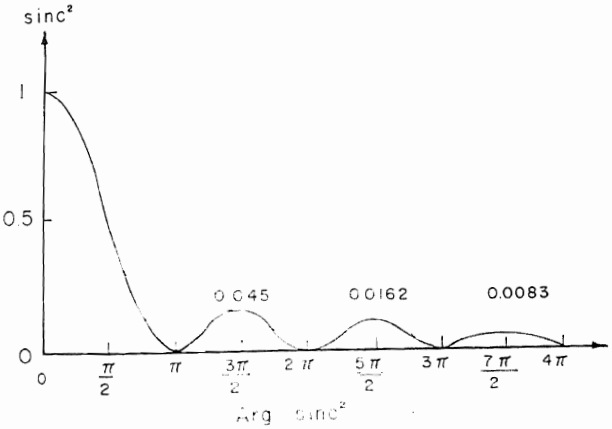

FIG. 9. Plot of the sinc² characteristic function.

VII. "REAL-TIME" HOLOGRAPHIC INTERFEROMETRY

Real-time holographic interferometry consists of taking a single-exposure hologram of an object in a given state and time, processing the emulsion, replacing the hologram exactly into the position in which it was recorded, illuminating the object with the same coherent (laser) light as during the recording, and using the coherent reference beam as the illuminating beam for the hologram. The virtual image, reconstructed by the hologram, then appears exactly superimposed onto the object behind the hologram! However, one can make a set of interference fringes cover the object (i.e., the virtual image), by causing the object to be suitably displaced with respect to the "superimposed" virtual image. The system of interference fringes results, in effect, from the interferometric comparison between the original state of the object (as materialized by the virtual image) and the state of the object at the instant of observation.

The interference fringes might be expected to be quite similar in "real-time" holographic interferometry, for the various cases, as it is in double-exposure and multiple-exposure ("time-average") holographic interferometry considered above. This is indeed found to be true for the observation of a nonmoving, statically displaced (or deformed) object through its own hologram. We also show, below, that the general appearance of the fringe system observed by looking at a vibrating object through its own hologram may be made quite similar to that observed with a "time-averaged" multiply exposed hologram. However, we find that the "real-time" fringes of vibrating objects have in practice much lower contrast than "time-average" fringes and that the law of intensity modulation is somewhat different.

Let us consider the theory of real-time fringe formation for the general case where the object undergoes both static displacement and harmonic vibration. Since the interference fringes are being observed in real time, we must first find the instantaneous intensity distribution and then time average this over the "integration" time of the human eye, recording camera, television receiver, and so on.

The instantaneous complex disturbance at the object may be written in the form

$$\mathbf{E}_{\text{image}}(\mathbf{r},t)=\mathbf{E}_O(\mathbf{r})\{1+\exp[i(\mathbf{m}_s\cdot\mathbf{k}'+\mathbf{m}\cdot\mathbf{k}'\sin\omega t]\}, \quad (70)$$

where $\mathbf{E}_O(\mathbf{r})$ represents the complex field in the reconstructed image from the single exposed hologram, as well as the complex field in the "static" original object state; $\mathbf{m}_s$ represents a static displacement of the object, independent of time; $\mathbf{m}\sin\omega t$ represents the harmonic motion vector, and where we have now written

$$\mathbf{m}=\mathbf{n}_m m,$$
$$\mathbf{k}'=\mathbf{k}_1+\mathbf{k}_2=(2\pi/\lambda)(\mathbf{n}_1+\mathbf{n}_2). \quad (71)$$

The phase term

$$\mathbf{E}_O(\mathbf{r})\{\exp[i(\mathbf{m}_s\cdot\mathbf{k}'+\mathbf{m}\cdot\mathbf{k}'\sin\omega t)]\}$$

in Eq. 70 represents the real object.

The instantaneous intensity in the object space is accordingly given by the equation

$$_{\text{mage}}(\mathbf{r},t)=[\mathbf{E}_O(\mathbf{r})\mathbf{E}_O(\mathbf{r})^*]\times\{2+\exp[i(\mathbf{m}_s\cdot\mathbf{k}'+\mathbf{m}\cdot\mathbf{k}'\sin\omega t)]+\exp[-i(\mathbf{m}_s\cdot\mathbf{k}'+\mathbf{m}\cdot\mathbf{k}'\sin\omega t)]\}. \quad (72)$$

The "time average" of this intensity over the integration time T is

$$\langle I_{\text{image}}(\mathbf{r},t)\rangle=I_O(\mathbf{r})\left[2+e^{i(\mathbf{m}_s\cdot\mathbf{k}')}\frac{1}{T}\int_0^T e^{i(\mathbf{m}\cdot\mathbf{k}'\sin\omega t)}dt+e^{-i(\mathbf{m}_s\cdot\mathbf{k}')}\frac{1}{T}\int_0^T e^{-i(\mathbf{m}\cdot\mathbf{k}'\sin\omega t)}dt\right], \quad (73)$$

which for $2\pi/\omega>T$ becomes (see preceding Sections) $\langle I_{\text{image}}(\mathbf{r},t)\rangle$

$$=I_O(\mathbf{r})[2+(e^{i(\mathbf{m}_s\cdot\mathbf{k}')}+e^{-i(\mathbf{m}_s\cdot\mathbf{k}')})J_0(\mathbf{m}\cdot\mathbf{k}')]$$
$$=2I_O(\mathbf{r})[1+\cos(\mathbf{m}_s\cdot\mathbf{k}')J_0(\mathbf{m}\cdot\mathbf{k}')]. \quad (74)$$

The fringe systems in "real-time" holographic interferometry may therefore readily be described as follows. For the case of *pure static displacement* with a displacement vector $\mathbf{m}_s$, and for which $\mathbf{m}=0$, the intensity in the image is

$$\langle I_{\text{image}}(\mathbf{r},t)\rangle=2I_O(\mathbf{r})[1+\cos(\mathbf{m}_s\cdot\mathbf{k}')], \quad (75)$$

the same as that given by Eq. 17 for the case of a doubly exposed hologram of a "statically moved" object!

On the other hand, for a harmonically vibrating object observed through its own hologram (in the case where the "static displacement" $\mathbf{m}_s$ is adjusted to be zero!), we find the intensity observed in the image to be (with $\mathbf{m}_s=0$)

$$\langle I_{\text{image}}(\mathbf{r},t)\rangle=2I_O(\mathbf{r})[1+J_0(\mathbf{m}\cdot\mathbf{k}')], \quad (76)$$

rather than

$$I_{\text{image}}(\mathbf{r})=I_O(\mathbf{r})|[J_0(\mathbf{m}\cdot\mathbf{k}')]|^2, \quad (77)$$

which is the intensity, according to Eq. 49 describing a "time-averaged" holographic interferogram. Aside from the fact that the Bessel function appears with its first power in Eq. 76 as compared to its square in Eqs. 49 and 77, the decrease in the contrast of the fringes is due to the additional unity term. In practice, the very noticeable "decrease" of fringe contrast in "real-time" holographic interferometry of vibrating objects, as compared to "time-average" holographic interferograms, is of course also further caused by the $\cos(\mathbf{m}_s\cdot\mathbf{k}')$ factor in Eqs. 74 and 75, which causes a reduction in fringe contrast, unless the "static displacement" vector $\mathbf{m}_s$ is adjusted to be equal to zero!

VIII. CONCLUSIONS

The theoretical results we have presented may serve as a basis for new theoretical and experimental departures—in the fields of acoustics and ultrasonics—that were not readily conceivable before the advent of holographic interferometry. Among these, one may mention immediate topological vibration-mode analysis of the entire surface of acoustical transducers, with the required optical precision in the microinch domain. Dramatic improvements in the possibilities of "beam shaping" of acoustical transducers thus also appear possible with the aid of a spatial Fourier-transform analysis of the topology of the vibrating transducers. These improvements in the "directivity" and efficiency of transducers may be obtained with the aid of holographic interferometry, along the lines already considered at the end of the last century by Lord Rayleigh and currently very fruitful in optical imaging. Significantly, the new field of holographic nondestructive testing (HNDT) has recently been applied to the inspection of pneumatic tires, sandwich structures, and other objects.